J|A|C|S
ARTICLES
Published on Web 01/19/2008

Development of an Efficient Photocatalytic System for CO_2 Reduction Using Rhenium(I) Complexes Based on Mechanistic Studies

Hiroyuki Takeda,[†] Kazuhide Koike,[‡] Haruo Inoue,[§,||] and Osamu Ishitani*[,†,||]

Department of Chemistry, Graduate School of Science and Engineering, Tokyo Institute of Technology, 2-12-1-E1-9 O-okayama, Meguro-ku, Tokyo, 152-8551, Japan, National Institute of Advanced Industrial Science and Technology, 16-1 Onogawa, Tsukuba, Ibaraki, 305-8569, Japan, Department of Applied Chemistry, Graduate Course of Urban Environmental Sciences, Tokyo Metropolitan University, 1-1 Minamiosawa, Hachioji, Tokyo, 192-0364, Japan, and SORST, Japan Science and Technology Agency (JST), Japan

Received October 9, 2007; E-mail: ishitani@chem.titech.ac.jp

Abstract: The reaction mechanism of photocatalytic CO_2 reduction using rhenium(I) complexes has been investigated by means of a detailed comparison of the photocatalyses of three rhenium(I) complexes, *fac*-[Re(bpy)$(CO)_3$L] (L = SCN^- (**1-NCS**), Cl^- (**1-Cl**), and CN^- (**1-CN**)). The corresponding one-electron-reduced species (OER) of the complexes play two important roles in the reaction: (a) capturing CO_2 after loss of the monodentate ligand (L) and (b) donation of the second electron to CO_2 by another OER without loss of L. In the case of **1-NCS**, the corresponding OER has both of the capabilities in the photocatalytic reaction, resulting in more efficient CO formation (with a quantum yield of 0.30) than that of **1-Cl** (quantum yield of 0.16), for which OER species have too short a lifetime to accumulate during the photocatalytic reaction. On the other hand, **1-CN** showed no photocatalytic ability, because the corresponding OER species does not dissociate the CN^- ligand. Based on this mechanistic information, the most efficient photocatalytic system was successfully developed using a mixed system with *fac*-[Re(bpy)$(CO)_3(CH_3CN)]^+$ and *fac*-[Re-{4,4′-$(MeO)_2$bpy}$(CO)_3${P$(OEt)_3$}$]^+$, for which the optimized quantum yield for CO formation was 0.59.

Introduction

Development of visible light driven photocatalysts for CO_2 reduction might provide a solution for both the shortage of fossil fuels and the global warming problem. It may give a new carbon source in place of fossil resources.

Although semiconductors such as TiO_2, ZnS, and CdS have been reported to act as photocatalysts for CO_2 reduction, their quantum yields and selectivities of products are low.[1−5] Photocatalytic systems, including transition metal complexes, such as ruthenium(II) polypyridine carbonyl complex,[6] cobalt(II) trisbipyridine,[7] and cobalt(III) macrocycles[8−10] as catalyst with a photosensitizer, can reduce CO_2 with relatively high quantum yield and high selectivity of products. In particular, the rhenium(I) bipyridine (bpy) complexes *fac*-$[Re^I(bpy)(CO)_3(L)]^{n+}$ (L = Cl (n = 0); PR_3 (n = 1)) have unique and high yield photocatalyses, so that they can work not only as a catalyst but also as a photosensitizer, and CO is the principal product of CO_2 reduction.[7,11−14] *fac*-[Re(bpy)$(CO)_3${P$(OEt)_3$}$]^+$ had previously been the most efficient photocatalyst for CO_2 reduction in a homogeneous system that selectively produces CO with a quantum yield of 0.38.[12] Many researchers have looked at the mechanism of CO_2 reduction using *fac*-$[Re^I(bpy)(CO)_3(L)]^{n+}$ as a photocatalyst.[13,15−21] The triplet metal-to-ligand charge

[†] Tokyo Institute of Technology.
[‡] National Institute of Advanced Industrial Science and Technology.
[§] Tokyo Metropolitan University.
[||] SORST.

(1) Inoue, T.; Fujishima, A.; Konishi, S.; Honda, K. *Nature* **1979**, *277*, 637−638.
(2) Thampi, K. R.; Kiwi, J.; Grätzel, M. *Nature* **1987**, *327*, 506−508.
(3) Ishitani, O.; Inoue, C.; Suzuki, Y.; Ibusuki, T. *J. Photochem. Photobiol. A: Chem.* **1993**, *72*, 269−271.
(4) Fujiwara, H.; Hosokawa, H.; Murakoshi, K.; Wada, Y.; Yanagida, S.; Okada, T.; Kobayashi, H. *J. Phys. Chem. B* **1997**, *101*, 8270−8278.
(5) Ikeue, K.; Yamashita, H.; Anpo, M.; Takewaki, T. *J. Phys. Chem. B* **2001**, *105*, 8350−8355.
(6) Ishida, H.; Terada, T.; Tanaka, K.; Tanaka, T. *Organometallics* **1990**, *6*, 181−186.
(7) Hawecker, J.; Lehn, J.-M.; Ziessel, R. *J. Chem. Soc., Chem. Commun.* **1983**, 536−538.
(8) Grodkowski, J.; Dhanasekaran, T.; Neta, P.; Hambright, P.; Brunschwig, B. S.; Shinozaki, K.; Fujita, E. *J. Phys. Chem. A* **2000**, *104*, 11332−11339.
(9) Ogata, T.; Yanagida, S.; Brunschwig, B. S.; Fujita, E. *J. Am. Chem. Soc.* **1995**, *117*, 6708−6716.
(10) Matsuoka, S.; Yamamoto, K.; Ogata, T.; Kusaba, M.; Nakashima, N.; Fujita, E.; Yanagida, S. *J. Am. Chem. Soc.* **1993**, *115*, 601−609.
(11) Hawecker, J.; Lehn, J.-M.; Ziessel, R. *Helv. Chim. Acta* **1986**, *69*, 1990−2012.
(12) Hori, H.; Johnson, F. P. A.; Koike, K.; Ishitani, O.; Ibusuki, T. *J. Photochem. Photobiol. A: Chem.* **1996**, *96*, 171−174.
(13) Koike, K.; Hori, H.; Ishizuka, M.; Westwell, J. R.; Takeuchi, K.; Ibusuki, T.; Enjouji, K.; Konno, H.; Sakamoto, K.; Ishitani, O. *Organometallics* **1997**, *16*, 5724−5729.
(14) Kurz, P.; Probst, B.; Spingler, B.; Alberto, R. *Eur. J. Inorg. Chem.* **2006**, 2966−2974.
(15) Kutal, C.; Weber, M. A.; Ferraudi, G.; Geiger, D. *Organometallics* **1985**, *4*, 2161−2166.
(16) Kutal, C.; Corbin, A. J.; Ferraudi, G. *Organometallics* **1987**, *6*, 553−557.
(17) Kalyanasundaram, K. *J. Chem. Soc., Faraday Trans.* **1986**, *2*, 2401−2415.
(18) Gibson, D. H.; Yin, X.; He, H.; Mashuta, M. S. *Organometallics* **2003**, *22*, 337−346.
(19) Gibson, D. H.; Yin, X. *Chem. Commun.* **1999**, 1411−1412.
(20) Hayashi, Y.; Kita, S.; Brunschwig, B. S.; Fujita, E. *J. Am. Chem. Soc.* **2003**, *125*, 11976−11987.

Table 1. Photophysical and Electrochemical Properties of the Rhenium(I) Complexes, and Reductive Quenching Rates of Their Emission by TEOA

	emission[a]			quenching by TEOA[a]		
	λ_{max}[b]		τ[d]	k_q[f]	$k_q\tau$	$E_{1/2}$[g]
complex	nm	Φ_f[c]	ns	$M^{-1}\,s^{-1}$	M^{-1}	V
1-NCS	635	0.003	30	3.7×10^8	11	−1.61
1-CN	611	0.013	87	2.5×10^8	22	−1.67
1-Cl	637	0.003	25[e]	8.0×10^7 [e]	2.1	−1.67

[a] Measured in DMF at room temperature under an Ar atmosphere. [b]Emission maxima. [c]Emission quantum yields. [d]Excited-state lifetimes. [e]Value measured in MeCN solution (ref 17). [f]Quenching rate constants of the emission by TEOA. [g]Redox potentials vs $Ag/AgNO_3$ (0.01 M) for (**1-x**/**1-x**$^{-\bullet}$).

transfer (^{3}MLCT) excited state of the rhenium complexes was quenched by tertiary amine (such as triethanolamine, TEOA) as the first step of the photocatalytic reaction, generating the one-electron reduced (OER) species of the rhenium complexes, in laser flush photolysis studies.[15−17] However, the following processes are not yet understood in detail: how the OER species react with CO_2, what is the second electron source for the two-electron reduction of CO_2 to CO, and how the photocatalyst is recovered after CO is produced.

There are some clues. In the photocatalytic reaction with *fac*-Re(bpy)$(CO)_3$Cl in the presence of Br^-, *fac*-Re(bpy)$(CO)_3$Br was formed.[7] On the other hand, under a $^{13}CO_2$ atmosphere, the complex converted to *fac*-Re(bpy)$(^{13}CO)_3$Cl during the photocatalytic reaction.[11] The OER species *fac*-[Re(bpy)$(CO)_3$-(PR_3)], which are produced by the photoinduced electron-transfer reaction with triethanolamine, reacted with CO_2 in the dark, with rate constants 3.5×10^{-4}−1.9×10^{-2} $M^{-1}\,s^{-1}$, and disproportionation of the OER species is not likely to be a major process for CO_2 reduction.[13] Some "CO_2 adducts" with reduced rhenium complexes, such as a CO_2-bridged rhenium dimer and metalocarboxylates, have been proposed as key intermediates for the photocatalytic reduction;[18−21] none of these complexes have been directly observed under photocatalytic reaction conditions.

We report below a detailed mechanistic study of photocatalytic CO_2 reduction using three rhenium(I) complexes with anionic ligand *fac*-[Re(bpy)$(CO)_3$(L)] (L = NCS^-, Cl^-, and CN^-) which have similar photophysical properties (shown in Table 1). This has clarified which ligand is eliminated from the OER species before reaction with CO_2, the identification of the second-electron donor, and how the starting complexes are reproduced in the photocatalytic cycle.

A most efficient homogeneous photocatalytic system has been developed by the molecular design of a new photocatalytic system based on the information about the reaction mechanism found in this study.

Experimental Section

General Procedures. IR spectra were recorded on a JASCO FT/IR-610 spectrometer at 2-cm^{-1} resolution. UV−vis absorption spectra were recorded on a JASCO V-565 or Photal MCPD-2000 photodiode-array spectrometer. The emission spectra were recorded with a JASCO FP6600 fluorescence spectrometer. ^{1}H NMR spectra were recorded on a Bruker AC200, JEOL EX270, or AL300 NMR spectrometer. Electrospray ionization mass spectra of the neutral complexes, using sodium ion as an ionization reagent,[22] were measured with an Applied Biosystems Mariner System 5231 mass spectrometer.

Materials. Acetonitrile was distilled three times over P_2O_5 and then distilled over CaH_2 just before use. Dimethylformamide (DMF) was dried over molecular sieves of size 4 Å and distilled at reduced pressure. Triethanolamine (TEOA) was distilled at reduced pressure. Tetraethylammonium tetrafluoroborate was prepared according to standard methods[23,24] and dried in vacuo at 100 °C for one night before use. Tetra-*n*-butylammonium thiocyanate and tetraethylammonium chloride were dried in vacuo at 100 °C for one night before use. The rhenium(I) complexes, *fac*-[Re(bpy)$(CO)_3$Cl] (**1-Cl**), *fac*-[Re(4,4′-Me_2bpy)$(CO)_3$Cl] (**1(Me)-Cl**), and *fac*-[Re(bpy)$(CO)_3(CH_3CN)](PF_6)$ (**[1-MeCN]**$^+$), were prepared according to standard methods.[25,26]

***fac*-[Re(bpy)$(CO)_3$(NCS)] (1-NCS).** An ethanol/water (1:1 v/v) mixed solution (300 mL) containing **1-Cl** (500 mg) and NaSCN (8.8 g) was refluxed under an Ar atmosphere for 12 h. The complex **1-NCS** was extracted from the reaction solution with CH_2Cl_2 three times. The resulting organic layer was washed with water and evaporated to give **1-NCS** as yellow solids. Purification of **1-NCS** was achieved by recrystallization with an acetone−water mix twice and then with acetone−Et_2O. The typical yield was 85%. ^{1}H NMR (270 MHz, acetone-d_6): δ/ppm, 7.87 (2H, ddd, J = 1.4 Hz, 5.6 Hz, 7.8 Hz, bpy H^5, $H^{5'}$), 8.42 (2H, ddd, J = 1.6 Hz, 7.8 Hz, 8.1 Hz, bpy H^4, $H^{4'}$), 8.76 (2H, ddd, J = 1.1 Hz, 1.1 Hz, 8.1 Hz, bpy H^3, $H^{3'}$), 9.15 (2H, ddd, J = 0.8 Hz, 1.6 Hz, 5.6 Hz, bpy H^6, $H^{6'}$). IR (MeCN): ν(CO)/cm^{-1}, 2027, 1919(br); ν(CN)/cm^{-1}, 2098. ESI-MS: m/z, 508 $[M + Na]^+$. UV−vis (CH_2Cl_2): λ_{max}/nm (ϵ / M^{-1} cm^{-1}), 297 (19700), 396 (2900). Anal. Calcd (%) for $C_{14}H_8O_3N_3SRe$: C, 34.71; H, 1.66; N, 8.67; S, 6.62. Found: C, 34.51; H, 1.61; N, 8.48; S, 6.73.

There are two linkage isomers with a SCN^- ligand, i.e., thiocyanato complex M−SCN and isothiocyanato complex M−NCS. Recently, **1-NCS** was synthesized by Vlček et al.[27] and was found to be the isothiocyanato isomer by X-ray single crystal analysis. The spectral and analytical data of **1-NCS** prepared in the present study were consistent with those reported by Vlček et al.[27]

***fac*-[Re(bpy)$(CO)_3$(CN)] (1-CN).** We prepared **1-CN** by modification of the method of that reported by Leasure et al., as follows.[28] An ethanol/water (1:1 v/v, 50 mL) mixture containing **[1-MeCN]**$^+(PF_6)^-$ (100 mg) and KCN (1.06 g) was refluxed under an Ar atmosphere for 6 h in dim light. The complex was extracted with CH_2Cl_2 three times, and the organic layer was washed with water three times. The solvent was evaporated, to give yellow solids. The complex **1-CN** was isolated by column chromatography on aluminum oxide with CH_2Cl_2/CH_3CN (3:1 v/v) eluent. Two bands appeared in the column; the first band contained **1-CN**. Further purification took place by recrystallization with an acetone−water mix twice and then with acetone−Et_2O. The yield was 64%. ^{1}H NMR (200 MHz, acetone-d_6): δ/ppm, 7.80 (2H, ddd, J = 1.0 Hz, 5.6 Hz, 7.6 Hz, bpy H^5, $H^{5'}$), 8.35 (2H, ddd, J = 1.4 Hz, 7.6 Hz, 8.5 Hz, bpy H^4, $H^{4'}$), 8.73 (2H, ddd, J = 1.0 Hz, 1.0 Hz, 8.5 Hz, bpy H^3, $H^{3'}$), 9.13 (2H, ddd, J = 1.0 Hz, 1.2 Hz, 5.6 Hz, bpy H^6, $H^{6'}$). IR (MeCN): ν(CO)/cm^{-1}, 2023, 1925, 1915; ν(CN)/cm^{-1}, 2124. ESI-MS: m/z, 476 $[M + Na]^+$. UV−vis (CH_2Cl_2): λ_{max}/nm (ϵ/$M^{-1}cm^{-1}$), 252 (16300), 287 (17400), 315 (7800), 374 (4000). Anal. Calcd (%) for $C_{14}H_8O_3N_3Re$: C, 37.17; H, 1.78; N, 9.29. Found: C, 37.37; H, 1.85; N, 9.15.

(21) Shinozaki, K.; Hayashi, Y.; Brunschwig, B. S.; Fujita, E. *Res. Chem. Intermed.* **2007**, *33*, 27−36.
(22) Hori, H.; Ishihara, J.; Koike, K.; Takeuchi, K.; Ibusuki, T.; Ishitani, O. *Chem. Lett.* **1997**, 273−274.
(23) Wheeler, Charles M. J.; Sandstedt, R. A. *J. Am. Chem. Soc.* **1955**, *77*, 2025−2026.
(24) Moe, N. S. *Acta Chem. Scand.* **1965**, *19*, 1023−1024.
(25) Caspar, J. V.; Meyer, T. J. *J. Phys. Chem.* **1983**, *87*, 952−957.
(26) Worl, L. A.; Duesing, R.; Chen, P.; Ciana, L. D.; Meyer, T. J. *J. Chem. Soc., Dalton Trans.* **1991**, 849−858.
(27) Rodríguez, A. M. B.; Gabrielsson, A.; Motevalli, M.; Matousek, P.; Towrie, M.; Sebera, J.; Záliš, S.; Anntonin. Vlček, J. *J. Phys. Chem. A* **2005**, *109*, 5016−5025.
(28) Leasure, R. M.; Sacksteder, L.; Nesselrodt, D.; Reitz, G. A.; Demas, J. N.; DeGraff, B. A. *Inorg. Chem.* **1991**, *30*, 3722−3728.

***fac*-[Re{4,4′-(MeO)$_2$bpy}(CO)$_3$Cl] (1(MeO)-Cl).** A toluene solution (50 mL) containing $Re(CO)_5Cl$ (0.30 g) and 4,4′-dimethoxy-2,2′-bipyridine (4,4′-(MeO)$_2$bpy) (0.19 g) was refluxed under an Ar atmosphere for 3 h in dim light. After the solution cooled to room temperature, the resulting yellow precipitates were filtered and washed with toluene, hot hexane, and then *n*-pentane. The yield was 0.40 g (93%). ^{1}H NMR (300 MHz, acetone-d_6): δ/ppm, 4.13 (6H, s, CH_3O), 7.29 (2H, dd, J = 2.7 Hz, 6.6 Hz, bpy H^5, $H^{5'}$), 8.17 (2H, d, J = 2.7 Hz, bpy H^3, $H^{3'}$), 8.83 (2H, d, J = 6.6 Hz, bpy H^6, $H^{6'}$). IR (MeCN): ν(CO)/cm^{-1}, 2020, 1913, 1893. Anal. Calcd (%) for $C_{15}H_{12}O_5N_2ClRe$: C, 34.52; H, 2.32; N, 5.37. Found: C, 34.53; H, 2.58; N, 5.62.

fac-[Re{4,4′-(MeO)$_2$bpy}(CO)$_3${P(OEt)$_3$}]$^+$(PF_6)$^-$ **([1(MeO)-P]$^+$-**(PF_6)$^-$). A tetrahydrofuran solution (50 mL) containing Re{4,4′-(MeO)$_2$bpy}(CO)$_3$Cl (0.30 g) and $Ag^+CF_3SO_3^-$ (0.15 g) was refluxed under an Ar atmosphere for 1.5 h in dim light. The precipitated silver chloride was filtered off, and triethyl phosphite (1 mL) was added to the filtrate. The solution was refluxed under an Ar atmosphere for 8 h in dim light. The solvent was evaporated, and the resulting yellow solids were washed several times with *n*-pentane. The salts were dissolved in methanol and a saturated methanolic solution of NH_4PF_6 was added, to give the PF_6^- salt of **[1(MeO)-P]**$^+$. Purification was achieved by recrystallization with CH_2Cl_2/Et_2O several times, with drying under vacuo. The yield was 0.46 g (70%). ^{1}H NMR (300 MHz, acetone-d_6): δ/ppm, 1.09 (9H, t, J = 7.1 Hz, POCH$_2$CH_3), 3.94 (6H, quint, J = 7.1 Hz, POCH_2CH$_3$), 4.16 (6H, s, CH_3O), 7.42 (2H, dd, J = 2.8 Hz, 6.5 Hz, bpy H^5, $H^{5'}$), 8.34 (2H, d, J = 2,8 Hz, bpy H^3, $H^{3'}$), 8.93 (2H, d, J = 6.5 Hz, bpy H^6, $H^{6'}$). IR (MeCN): ν(CO)/cm^{-1}, 2044, 1956, 1923. ESI-MS: m/z, 653 [M− PF_6^-]$^+$. UV−vis (CH_2Cl_2): λ_{max}/nm (ϵ/M^{-1}-cm^{-1}), 251 (33900), 294sh (10300), 301 (9260), 336 (5090). Anal. Calcd (%) for $C_{21}H_{27}O_8N_2P_2F_6Re$: C, 31.62; H, 3.41; N, 3.51. Found: C, 31.71; H, 3.51; N, 3.56.

Electrochemistry. Cyclic voltammograms were measured in an acetonitrile solution containing complex (0.5 mM) and Et_4NBF_4 (0.1 M) as the supporting electrolyte under an Ar atmosphere. We used a BAS CHI620 electrochemical analyzer with a glassy-carbon working electrode (diameter 3 mm), a Ag/$AgNO_3$ (0.01 M) reference electrode, and a Pt counter electrode at a scan rate of 100 mV s^{-1}.

Flow electrolysis[29] was used to measure IR and UV−vis absorption spectra of the OER species of the complexes. The working electrode was contained in a porous glass tube (2 mm *i.d.*, 3 mm *o.d.*, 40 mm length) and consisted of many strands of 0.1 mm diameter Pt wire. The counter electrode was a Pt wire coiled around the porous glass tube. The I_2/I_3^- reference electrode, which consists of a Pt wire and an acetonitrile solution containing 0.1 M I_2 and 0.1 M Et_4NI, was equipped near the counter electrode. An acetonitrile solution containing a rhenium complex (0.5 mM), and Et_4NBF_4 (0.1 M) as electrolyte, was purged with Ar for 20 min and was then passed into the flow-through cell at a rate of 0.5 mL/min using a JASCO PU-980 pump. Immediately after electrolysis using a BAS CHI 620 electrochemical analyzer, the solution was transferred to a CaF_2 cell (path length ca. 1.5 mm) and/or a quartz cell (path length 1.5 mm) for spectral measurements.

Photocatalytic Reactions. A 4-mL DMF− TEOA (5:1 v/v) solution containing a rhenium complex in a pyrex test tube (*i.d.* = 8 mm; 11.4 mL volute) or a quartz cubic cell (1-cm pass length; 11.0 mL volume) was bubbled through with CO_2 for 20 min. The pyrex test tubes were equipped with a merry-go-round apparatus with a 500-W high-pressure mercury lamp and a solution cutoff filter (<330 nm; 1-cm path length); this is a 300 mL aqueous solution containing $NiSO_4$·$6H_2O$ (75 g) and $CoSO_4$·$7H_2O$ (72 g).

To determine the quantum yield of a photochemical reaction, or to record spectral changes of the reaction solution, the sample solution (in a quartz cubic cell) was irradiated using an Ushio Optical Moduley high-pressure Hg lamp BA-H500 with a 365-nm band-pass filter (fwhm = 10 nm) purchased from Asahi Spectra Co. and a $CuSO_4$ solution (250 g l^{-1}, 5-cm pass length) filter. Neutral density (ND) glass filters were used in order to reduce the light intensity. The temperature of the reaction solution was maintained at 25 ± 0.2 °C using a TAITEC LabBath LB-21JR cooling thermo pump during the irradiation. The incident light intensity was determined using a $K_3[Fe(C_2O_4)_3]$ actinometer.[30] The gaseous reaction products, i.e., CO and H_2, were analyzed using GC-TCD (Shimadzu GC-9A) with an active carbon column. Quantum yields for CO formation were calculated as the number of CO molecules formed, divided by the number of absorbed photons. The complexes were analyzed using an HPLC system with a Shimadzu LC-10AD pump, a Nomura ODS-HG-5 column (25 cm), a Shimadzu SPD-10AV detector (wavelength 320 nm), and a Rheodyne 7125 injector. The mobile phase was a mixture (3:2 v/v) of MeOH and a KH_2PO_4−NaOH buffer solution (0.05 M, pH 5.9). The anions in the solution were analyzed using an Otsuka Electronics CAPI-3300I Photal capillary electrophoresis system with a buffer solution (pH 8.5) consisting of ammonium molybdate, diethylenetriamine, and trishydroxyaminomethane as the electrolyte.

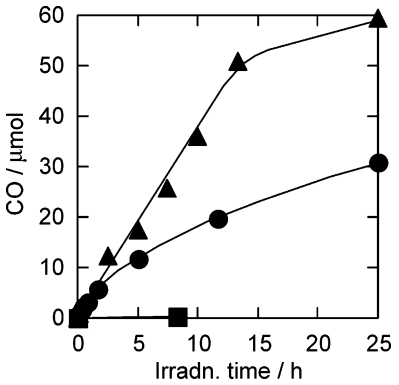

Figure 1. Irradiation-time dependence of CO formation using **1-NCS** (▲), **1-Cl** (●), and **1-CN** (■): irradiation with 365-nm light to a 4-mL DMF−TEOA (5:1 v/v) solution containing the complex (0.5 mM) under a CO_2 atmosphere, with light intensity 8.5 × 10^{-9} einstein s^{-1}.

^{13}C NMR Study of Photocatalytic CO_2 Reduction. A DMF-d_6−TEOA (1:5 v/v) solution (0.5 mL) containing **1-NCS** (30 mM) was degassed by the freeze−pump−thaw method and transferred into an NMR tube (total volume ∼4 mL; i.d. = 5 mm). After 0.72 atm of ^{13}CO gas (^{13}C content 99.8 atom%) was introduced through a vacuum line, the NMR tube was shaken for several minutes and the tube was sealed with a flame torch. The solution was irradiated with the merry-go-round apparatus described above. The ^{13}C NMR spectra of the solution after 24-h irradiation were measured on a JEOL Lambda 500 system (125.65 MHz), using DMF-d_6 as an internal standard. Integration of the peaks obtained by the NOE complete ^{1}H-decoupling method (EXMOD: nne) was used to determine the relative concentrations of the ^{13}CO ligands. The carbons in the bpy ligand were used as an internal standard.

Results and Discussion

Photocatalyses. Figure 1 shows the amounts of CO formed in the photocatalytic CO_2 reduction using **1-NCS**, **1-Cl**, and **1-CN**. It is clear that the photocatalytic activities of these three complexes are very different. In the case of **1-NCS**, 60 μmol of CO were produced after 25 h of irradiation, whereas **1-Cl** produced only 30 μmol of CO under the same conditions.

(29) Ishitani, O.; George, M. W.; Ibusuki, T.; Johnson, F. P. A.; Koike, K.; Nozaki, K.; Pac, C.; Turner, J. J.; Westwell, J. R. *Inorg. Chem.* **1994**, *33*, 4712−4717.

(30) Calvert, J. G.; Pitts, J. N. *Photochemistry*; Wiley and Sons: NewYork, 1966.

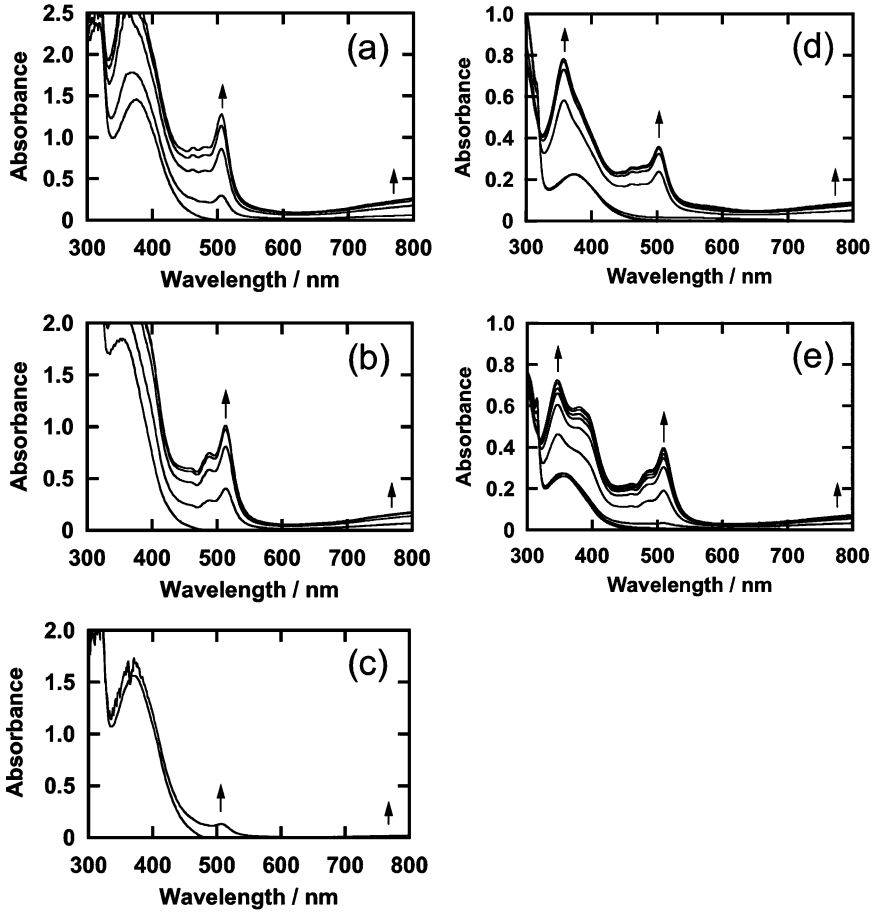

Figure 2. At left, UV−vis spectra changes of DMF−TEOA (5:1 v/v) solutions of (a) **1-NCS**, (b) **1-CN**, and (c) **1-Cl** (0.5 mM) during irradiation with 365-nm monochromic light under a CO_2 atmosphere (before the irradiation; ∼1 s; 5 s; 10 s; 15 s). At right, UV−vis spectral changes of CH_3CN solutions containing (d) **1-NCS** and (e) **1-CN** (0.5 mM) with 0.1 M Et_4NBF_4 during flow electrolysis under an Ar atmosphere. The following potentials vs $Ag/AgNO_3$ (0.01 M) were employed: (d) before the electrolysis; −1.35; −1.55; −1.65; −1.70; −1.75; −1.80 V and (e) before the electrolysis; −1.25; −1.45; −1.50; −1.65; −1.70; −1.75; −1.80; −1.85; −1.95; −2.00 V. The arrows indicate increasing absorbance.

However, **1-CN** cannot act as a photocatalyst.[31] The turnover numbers for CO formation (TN_{CO}) were 30 and 15 using **1-NCS** and **1-Cl**, respectively. The quantum yields of CO formation (Φ_{CO}) were 0.30 (**1-NCS**) and 0.16 (**1-Cl**), where the concentration of the complex was 2.5 mM and the light intensity was 7.5×10^{-9} einstein s^{-1}; the incident light was almost completely absorbed by the complex. Only small amounts of H_2 (less than 0.1 μmol) were formed in all cases.

Photochemical Production and Reactivities of One-Electron-Reduced Species. Figure 2a shows the UV−vis absorption spectral change of the reaction solution containing **1-NCS** during the photocatalytic reaction. A sharp absorption band near 500 nm, and a broad band in the near IR region, appeared just after irradiation commenced. These new bands were characteristic for the anion radical for the bpy ligand ($bpy^{-\bullet}$), and a very similar absorption spectrum was observed by the quantitative one-electron reduction of **1-NCS** using a flow-electrolysis technique, as shown in Figure 2d. Consequently, the one-electron reduced (OER) species of **1-NCS**, *fac*-$[Re(bpy^{-\bullet})(CO)_3(NCS)]^-$, should be produced in the first stage of the photocatalytic reaction. Similar results were obtained using **1-CN** (Figure 2b and 2e) instead of **1-NCS**.

As shown in Table 1, the ^{3}MLCT excited states of both **1-NCS** and **1-CN** are efficiently quenched by TEOA. Reductive quenching of the excited state should therefore give the OER species of these complexes. Although similar reductive quenching has been reported in the case of **1-Cl**, a far smaller amount of the OER species accumulated in the reaction solution even in the first stage of the photocatalytic reaction, as shown in Figure 2c, because of the much lower stability of the OER species of **1-Cl** than of the other complexes.

The reactivities of the OER species of both **1-NCS** and **1-CN** with CO_2 were investigated as follows. The OER species were produced by photoirradiation (1.0×10^{-7} einstein s^{-1}) of a DMF solution containing the complex in the presence of TEOA (1.26 M) for 20−90 s under CO_2, CO_2−Ar (1 : 1), or Ar. Immediately after stopping irradiation, the decay profiles of the OER species were followed in the dark by measuring the absorbance at 506 nm, a wavelength which can be absorbed by the OER species but not by the starting complexes. Figure 3 shows the results for **1-NCS**. The decay rate of the OER species of **1-NCS** increased in the presence of higher concentrations of CO_2: we found that $\tau_{1/2} = 98$ s under Ar, 49 s under CO_2−Ar (1:1) mixture, and 39 s under CO_2. Decay of the OER species of **1-Cl** was also accelerated in the presence of CO_2: $\tau_{1/2} = 39$ s

(31) Although photocatalysis of **1-CN** which was produced in the photoreaction of *fac*-$[Re(bpy)(CO)_3(4\text{-cyanopyridine})]^+$ with TEOA under a CO_2 atmosphere has been reported, it is clear that very pure **1-CN** has no photocatalytic activity. A small amount of other complex(es) should work as a catalyst for CO_2 reduction: Hori, H.; Ishihara, J.; Koike, K.; Takeuchi, K.; Ibusuki, T.; Ishitani, O. *J. Photochem. Photobiol. A: Chem.* **1999**, *120*. 119−124.

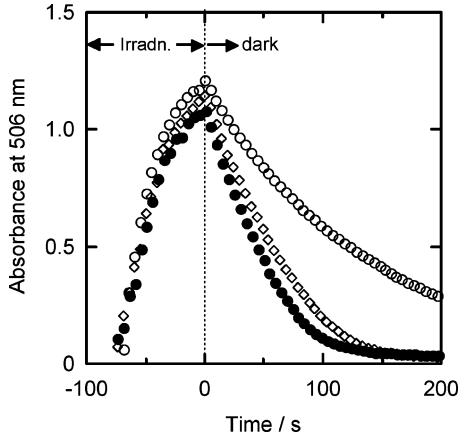

Figure 3. Decay curves of the absorbance at 506 nm of DMF−TEOA (5:1 v/v) solutions with **1-NCS** (0.5 mM) under Ar (○), CO_2−Ar (1:1) (◇), and CO_2 atmosphere (●) after irradiation with 365-nm monochromic light having intensity of 1.0×10^{-8} einstein s^{-1}.

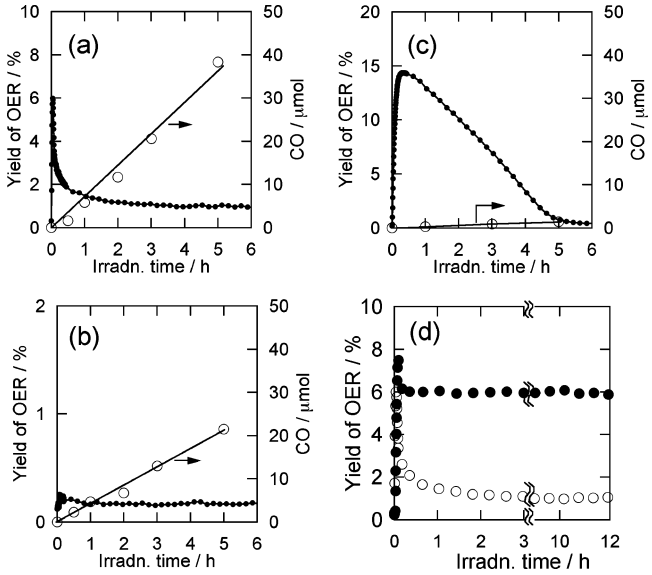

Figure 4. Yields of the OER species of the complex (●) and CO (○) during photocatalytic reactions using (a) **1-NCS**, (b) **1-Cl**, and (c) **1-CN** (2.5 mM) with 365-nm monochromic light (intensity 7.5×10^{-9} einstein s^{-1}) under a CO_2 atmosphere. (d) Comparison of yields of OER of **1-NCS** in the absence (○) and presence (●) of *n*-Bu_4NSCN (50 mM), where the reaction conditions were as described above.

under Ar and < 1 s under CO_2. In contrast, the decay of the OER species of **1-CN** was not affected by CO_2.

These results clearly show that the photochemical formation rates of all three OER complexes are similar (eq 1), but their decay profiles are quite different, i.e., **[1-NCS]**$^{-\bullet}$ and **[1-CN]**$^{-\bullet}$ are relatively stable in the dark and accumulate in solution, but **[1-Cl]**$^{-\bullet}$ is not stable; also, **[1-NCS]**$^{-\bullet}$ and **[1-Cl]**$^{-\bullet}$ can react with CO_2, but **[1-CN]**$^{-\bullet}$ does not.

$$fac\text{-}[Re(bpy)(CO)_3L] \xrightarrow[\text{in DMF/TEOA (5:1 v/v)}]{h\nu} fac\text{-}[Re(bpy^{-\bullet})(CO)_3L]^- \quad (1)$$

Figure 4 shows the time profiles of the amount of the OER species, during the photocatalytic reactions. Note the experimental differences between Figures 3 and 4: the former was obtained in the dark immediately after brief irradiation, whereas for the latter the solution was continuously irradiated. For both **1-NCS** and **1-CN** the corresponding OER species accumulated immediately after a short period of irradiation, as described above. The behavior of the OER species varied. Further irradiation caused a rapid decrease of **[1-NCS]**$^{-\bullet}$ to one-sixth of the maximum amount after 3 min of irradiation, but a photostationary state of **[1-NCS]**$^{-\bullet}$ was reached after 30 min of irradiation. After that, a very slow decrease of **[1-NCS]**$^{-\bullet}$ occurred, but **[1-NCS]**$^{-\bullet}$ was still observed until CO formation ceased (Figure 4a). The rapid decrease of **[1-NCS]**$^{-\bullet}$ in the first stage of the photoreaction should correspond to elimination of the SCN^- ligand, because addition of excess SCN^- caused a dramatic increase of **[1-NCS]**$^{-\bullet}$ in the photostationary state (Figure 4d). No comparable rapid decrease of **[1-CN]**$^{-\bullet}$ was observed in the first stage of the photoreaction, but **[1-CN]**$^{-\bullet}$ decreased gradually during 5 h of irradiation (Figure 4c). The accumulation and decrease of **[1-Cl]**$^{-\bullet}$ were similar to those of **[1-NCS]**$^{-\bullet}$, but the amount that accumulated in the photostationary state was much less (Figure 4b).

There have been reports of the dissociation of a ligand from OERs of rhenium diimine complexes in electrospectroscopic studies. Stufkens et al.[32] shows that the elimination capabilities of ligands from the OER species is in the order halide ≫ PPh_3, *n*-PrCN > $P(OMe)_3$ that corresponds to the order of weakness of π acceptabilities of the ligands. Kaim et al.[33] looked at the electron paramagnetic resonance spectroscopy of **[1-Cl]**$^{-\bullet}$ and suggested that the dissociation of Cl^- from **[1-Cl]**$^{-\bullet}$ is due to the electron density population on the Re−Cl dσ* orbital, through hyperconjugation from bpy π*. Bignozzi et al.[34] reported the CV behavior of **1-CN** and **1-Cl** at low temperature and concluded that, at low temperature, the doubly reduced species of **1-Cl** eliminates Cl^-, whereas that of **1-CN** does not eliminate CN^-. They pointed out that the difference in the reactivities is attributable to the different energies of the Re−L dσ* orbitals, i.e., dσ*(Cl^-) < dσ*(CN^-), because the CN^- ligand induces stronger ligand field splitting. The stability of **[1-NCS]**$^{-\bullet}$ is between that of **[1-Cl]**$^{-\bullet}$ and **[1-CN]**$^{-\bullet}$, probably because of its moderate ligand field and π acceptability.

Change of the Rhenium Complexes during Photocatalytic Reactions. The rhenium complexes in the solutions before and after the photocatalytic reaction were analyzed using high-performance liquid chromatography (Figure S1 in the Supporting Information). In all cases the peaks of the original complexes decreased, and new peaks appeared. For both **1-NCS** and **1-Cl**, the new peaks were observed at retention times of 6.7, 7.1, and 8.6 min, which were attributed to $[Re(bpy)(CO)_3(DMF)]^+$, $[Re(bpy)(CO)_3(TEOA)]^+$, and $[Re(bpy)(CO)_3(O_2CH)]$, respectively.[35] In the same solutions, free SCN^- and Cl^- were detected by capillary electrophoresis (CE). Figure 5a shows the time profiles of CO formation, the decrease of **1-NCS**, and the formation of free SCN^- during the photocatalytic reaction. A rapid decrease of **1-NCS** was observed within 1 h of irradiation, followed by a much slower decrease. The amount of free SCN^- was almost the same as that of the decrease of the starting complex. Similar phenomena were observed in the case of **1-Cl**, but the decrease of **1-Cl** was more rapid, and the amount of

(32) Stor, G. J.; Hartl, F.; van Outersterp, J. W. M.; Stufkens, D. J. *Organometallics* **1995**, *14*, 1115−1131.
(33) Klein, A.; Vogler, C.; Kaim, W. *Organometallics* **1996**, *15*, 236−244.
(34) Paolucci, F.; Marcaccio, M.; Paradisi, C.; Roffia, S.; Bignozzi, C. A.; Amatre, C. *J. Phys. Chem. B* **1998**, *102*, 4759−4769.
(35) Hori, H.; Johnson, F. P. A.; Koike, K.; Takeuchi, K.; Ibusuki, T.; Ishitani, O. *J. Chem. Soc., Dalton Trans.* **1997**, 1019−1023.

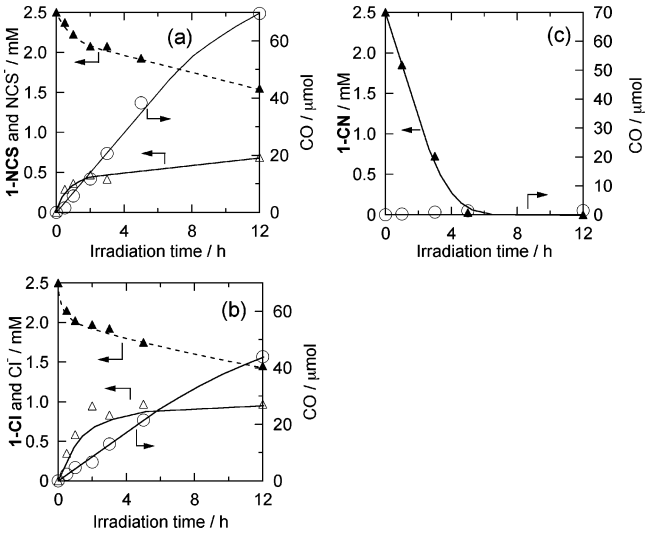

Figure 5. Irradiation time dependence of CO formation (○), and amounts of the starting complex (▲) and the dissociated anion (△) in the reaction solutions containing (a) **1-NCS**, (b) **1-Cl**, and (c) **1-CN**. A 4-mL DMF−TEOA (5:1 v/v) solution was used containing 2.5 mM of the complex using 365-nm monochromic light at a high intensity of 7.25×10^{-9} einstein s^{-1} under a CO_2 atmosphere.

residual **1-Cl** after 1 h of irradiation was less than that with **1-NCS** (Figure 5b). On the other hand, no such rapid decrease was observed in the case of **1-CN**, which decreased gradually during 5 h of irradiation, as shown in Figure 5c. Although new peaks were observed in the chromatogram of the solution after 1 h of irradiation, the solvent complexes and the formate complex were not detected in the case of **1-CN** (Figure S1c in the Supporting Information). Free CN^- was not detected at all by CE analysis. These results clearly indicate that elimination of the CN^- ligand does not occur from **[1-CN]**$^{-\bullet}$ under the photocatalytic reaction conditions. The yellow color of the solution, attributed to **1-CN**, was bleached after 5 h of irradiation, but three ν(CO) stretching bands were still observed in the FT-IR spectrum. Structural changes of the bpy ligand, such as reduction and elimination, may occur during irradiation.

The observed behaviors of the complexes and of the corresponding OER species clearly show that the SCN^- and Cl^- ligands are eliminated from **[1-NCS]**$^{-\bullet}$ and **[1-Cl]**$^{-\bullet}$, respectively, in the first stage of the photocatalytic reactions, while elimination of CN^- from **[1-CN]**$^{-\bullet}$ does not occur; there should be other relatively slow decomposition processes of **[1-CN]**$^{-\bullet}$ (eq 2). The equilibrium, shown in eq 3, should be achieved by further irradiation in the cases of **1-NCS** and **1-Cl**, because of the appearance of the photostationary states of **1-NCS**, **1-Cl** (Figure 5), and the corresponding OER species (Figure 4).

$$\textbf{1-CN} \xrightarrow[\text{TEOA}]{h\nu} \textbf{[1-CN]}^{-\bullet} \xrightarrow{\text{Other decomposition processes}} \textbf{1} + CN^- \quad (2)$$

$$\textbf{1-X} \xrightarrow[\text{TEOA}]{h\nu} \textbf{[1-X]}^{-\bullet} \rightleftharpoons \textbf{1} + X^- \quad (X = SCN^-, Cl^-) \quad (3)$$

The following evidence strongly supports the hypothesis that **1** reacts with CO_2 to give CO but the **[1-X]**$^{-\bullet}$ (X = SCN^-, Cl^-) does not:

1. The presence of an excess amount of SCN^- in the reaction solution did not increase the CO formation, but a dramatic increase of **[1-NCS]**$^{-\bullet}$ was observed at the photostationary state (Figure 4d).

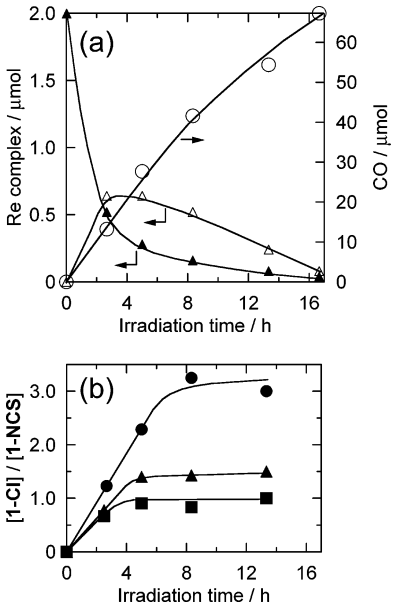

Figure 6. (a) Irradiation−time dependence of CO formation (○), and amounts of **1-NCS** (▲) and **1-Cl** (△) in the photocatalytic reaction solution in the presence of Cl^-; a 4-mL DMF−TEOA (5:1 v/v) solution containing **1-NCS** (0.5 mM) and Et_4NCl (10 mM) was irradiated under a CO_2 atmosphere. (b) Ratios of concentrations of **1-Cl** and **1-NCS** in the photocatalytic reaction solution in the presence of *n*-Bu_4NSCN, 0.5 mM (▲) and 1.0 mM (■), and in its absence (●). The reaction conditions were the same as above.

2. The decrease of **[1-NCS]**$^{-\bullet}$ under CO_2 in the dark became slower in the presence of excess SCN^-: $\tau_{1/2} = 39$ s in the absence of SCN^-, but $\tau_{1/2} = 64$ and 83 s in the presence of 50 and 100 mM SCN^-. On the other hand, no slow decrease of **[1-NCS]**$^{-\bullet}$ was observed in the presence of 100 mM $Et_4N^+BF_4^-$.

3. Although **1-CN** is efficiently reduced under the photocatalytic reaction conditions to give **[1-CN]**$^{-\bullet}$, elimination of CN^- from **[1-CN]**$^{-\bullet}$ does not occur, and **1-CN** cannot function as a photocatalyst for CO_2 reduction.

Although the elimination of Cl^- is a key step of electrocatalytic reduction of CO_2 by *fac*-Re(bpy)$(CO)_3$Cl,[36,37] the present observations constitute the first evidence that reaction of **1** with CO_2 causes CO formation in the photocatalytic reaction.

Fujita et al. reported the reactivity with CO_2 of [Re(bpy$^{-\bullet}$)$(CO)_3$], made by photoirradiation to $[Re(bpy)(CO)_3]_2$.[20,21] Their results show that [Re(bpy$^{-\bullet}$)$(CO)_3$] rapidly accommodates a solvent molecule (S) such as THF and CH_3CN to produce [Re(bpy$^{-\bullet}$)$(CO)_3$S], in which the unpaired electron is located mainly on the bpy ligand. The reaction rate of [Re(bpy$^{-\bullet}$)$(CO)_3$S] with CO_2 was relatively slow ($k_{obs} \approx 0.003$ s^{-1} under 0.8 atm of CO_2) in THF.

It follows that the OER species **[1-NCS]**$^{-\bullet}$ and **[1-Cl]**$^{-\bullet}$, which were formed via reductive quenching of the ^{3}MLCT excited state by TEOA, dissociates into X^- (SCN^- and Cl^-) and the OER species of the solvento complexes [Re(bpy$^{-\bullet}$)$(CO)_3$S] (S = DMF, TEOA), and the OER species of the solvento complexes should react with CO_2.

It is again noteworthy that, although the solvento complexes and a small amount of the formate complex [Re(bpy)$(CO)_3$-

(36) Sullivan, B. P.; Bolinger, C. M.; Conrad, D.; Vining, W. J.; Meyer, T. J. *J. Chem. Soc., Chem. Commun.* **1985**, 1414−1416.
(37) Johnson, F. P. A.; George, M. W.; Hartl, F.; Turner, J. J. *Organometallics* **1996**, *15*, 3374−3387.
(38) New peaks at 198.6, 194.8, 198.3, 194.2, and 191.2 ppm were observed but have not yet been identified.

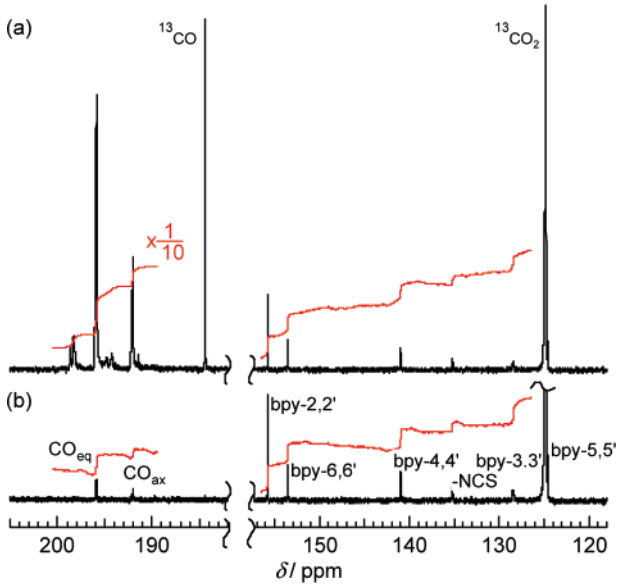

Figure 7. ^{13}C NMR spectra of a DMF-d_7−TEOA (5:1 v/v) solution containing **1-NCS** (30 mM) (a) after and (b) before 24 h of irradiation under a $^{13}CO_2$ (0.72 atm) atmosphere.[38] Integration curves are shown as red lines. The spectra were recorded under the following conditions: EXMODE nne: acquisition time 2.4 s; pulse delay 5 s; 10 000 times integration. The solution was irradiated using a merry-go-round apparatus with a high-pressure mercury lamp and the solution filter described in the Experimental Section.

(OCHO)] were generated during the photocatalytic reaction using **1-NCS** and **1-Cl**, these complexes have only low photocatalytic ability: $\Phi_{CO} = 0.04$ for the solvento complexes, and $\Phi_{CO} = 0.05$ for the formate complex.[35] This is because the excited-state lifetimes of these species are too short to be photochemically reduced by TEOA. Consequently, a recovering process of the starting complex, **1-NCS** or **1-Cl**, is necessary for efficient photocatalytic CO_2 reduction (eq 4). Formation of

$$[\mathrm{Re(bpy^{-\bullet})(CO)_3}] + \mathrm{L} \xrightarrow[e^-]{CO_2 \quad CO} \textit{fac}\text{-}[\mathrm{Re(bpy)(CO)_3L}] \quad (4)$$

$$(\mathrm{L} = \mathrm{Cl^-}, \mathrm{SCN^-})$$

the solvento complexes should be a competitive process versus the recoordination of SCN^- and Cl^- to the rhenium complex. Accordingly, both dissociation and recoordination abilities of the anionic ligands strongly affect the photocatalysis.

Figure 6a shows the effects of addition of Cl^- (10 mM) on the photocatalytic reaction by **1-NCS** (0.5 mM). In the first stage of the photocatalytic reaction, **1-Cl** formed but **1-NCS** decreased (see Figure 6a). After 5 h of irradiation, a photostationary state between **1-NCS** and **1-Cl** was reached, in the ratio 1:3 as shown in Figure 6b. Although further irradiation caused a gradual decrease of the complexes, CO was formed continuously in proportion to the total amount of **1-NCS** and **1-Cl** (Figure 6a). The addition of small amounts of SCN^- (0.5 and 1.0 mM) caused a dramatic decrease of the population of **1-Cl** in the photostationary state (Figure 6b). The ratio [**1-Cl**]/[**1-NCS**] in the photostationary state was proportional to the ratio of the anions $[Cl^-]/[SCN^-]$ (Figure S2 in the Supporting Information), and the gradient was 0.16. Addition of excess Cl^- did not affect the concentration of **[1-NCS]**$^{-\bullet}$ in the photostationary state (Figure S3 in the Supporting Information). These results indicate that the ability of Cl^- to coordinate to the rhenium center is

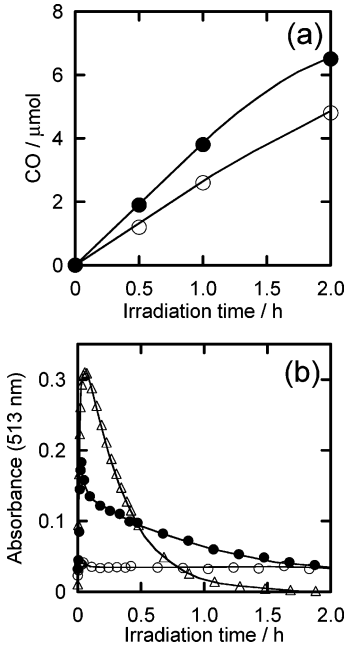

Figure 8. (a) Photocatalytic CO formation (●) by a mixed system of **1-(Me)-Cl** (0.11 mM) and **1-CN** (0.11 mM) and (○) by only **1(Me)-Cl** (0.11 mM) in the presence of Et_4NCl (11 mM). (b) Changes in absorbance of reaction solutions at 513 nm during irradiation; 4-mL DMF−TEOA (5:1 v/v) solutions containing (○) **1(Me)-Cl** (0.11 mM) and Et_4NCl (11 mM), (●) **1(Me)-Cl** (0.11 mM), **1-CN** (0.11 mM), and Et_4NCl (11 mM), and (△) **1-CN** (0.11 mM) and Et_4NCl (11 mM) were irradiated under CO_2 by 365-nm monochromic light of intensity 7.25×10^{-9} einstein s^{-1}.

Scheme 1

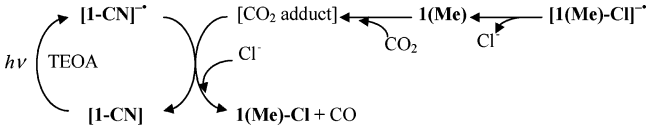

much less than that of SCN^-. It is noteworthy that **1-Cl** did not form by dark reaction of Cl^- with *fac*-$[Re(bpy)(CO)_3(DMF)]^+$ and *fac*-$[Re(bpy)(CO)_3(TEOA)]^+$ in a DMF−TEOA mixed solution. There are two possible formation processes of **1-Cl** during the photocatalytic reaction involving **1-NCS** in the presence of Cl^-: (1) coordination of Cl^- to **1** produced by elimination of SCN^- from **[1-NCS]**$^{-\bullet}$; (2) coordination of Cl^- immediately after elimination of CO from the rhenium center. Since **[1-Cl]**$^{-\bullet}$ is too unstable to accumulate during the photocatalytic reaction, process (1) is probably minor.

Figure 7 shows ^{13}C NMR spectra of a DMF-d_7−TEOA solution containing **1-NCS** before and after irradiation for 24 h. We observe two important facts: (a) CO_2 is the main source of CO, and (2) the three CO ligands are quantitatively substituted with ^{13}CO formed from $^{13}CO_2$ during irradiation. GC analysis of the gas phase in the NMR tube after irradiation shows that TN_{CO} was 2.5, while 25% of the **1-NCS** disappeared. Lehn and co-workers have reported similar phenomena with **1-Cl** photocatalyst.[11] The rhenium dimer with CO_2 as a bridge ligand $[Re(bpy)(CO)_3\text{-}C(O)O\text{−}Re(bpy)(CO)_3]$ and the carboxylate complex $[Re(bpy)(CO)_3(COOH)]$ have been proposed as a precursor for CO formation. However, the experimental results using $^{13}CO_2$ indicate that simple CO elimination from the bridge CO_2 or carboxylate ligand are not the main processes in the photocatalytic reaction. These ligands should be converted to a CO ligand before CO formation.

Scheme 2. Photocatalytic Reaction Mechanism by **1-NCS**

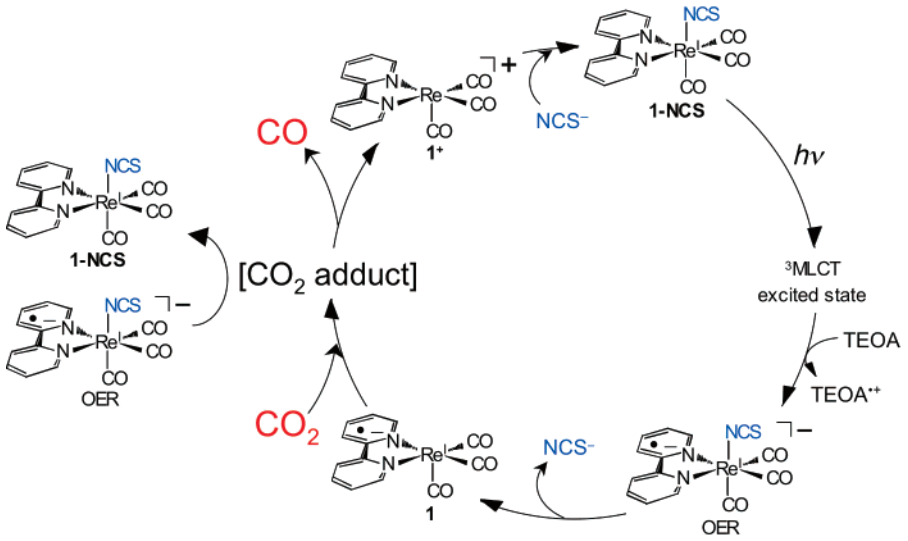

As described above, **1-NCS** has much greater photocatalytic ability than **1-Cl**. However, elimination of the Cl^- anion from **[1-Cl]**$^{-\bullet}$ is much more efficient than that of SCN^- from **[1-NCS]**$^{-\bullet}$, both of which give **1**, the precursor of CO_2 reduction. In addition, **[1-NCS]**$^{-\bullet}$ accumulated during the photocatalytic reaction, whereas only a small amount of **[1-Cl]**$^{-\bullet}$ accumulated even in the initial stage of the photoreaction. These results suggest that the OER of **1-NCS** is not only the precursor of **1** but plays a further role in the photocatalytic reduction of CO_2. We infer that its role is as an electron donor to the CO_2 adduct which should be produced by the reaction of **1** with CO_2, because CO is the two-electron reduced product of CO_2 but **1** has only a single extra electron. The following experiments found that the OER species can function as an electron donor for CO_2 reduction.

A DMF−TEOA (5:1 v/v) solution containing an equimolar amount (0.11 mM) of both *fac*-[Re(4,4′-Me_2bpy)$(CO)_3$Cl] (**1-(Me)-Cl**) and **1-CN** was irradiated under a CO_2 atmosphere. The photocatalytic activity of the mixed system was 1.2 times higher than that of the system containing only **1(Me)-Cl** (0.22 mM) (Figure 8a). On the other hand, accumulation of **[1-CN]**$^{-\bullet}$ in the mixed system during irradiation was almost half that using only **1-CN** (Figure 8b). As described above, **1-CN** cannot act as a photocatalyst for CO_2 reduction by itself. The OER species of **1-CN** is unable to reduce **1(Me)-Cl** because it has a lower redox potential (Table 1) than **1(Me)-Cl** ($E_{1/2} = -1.77$ V vs $Ag/AgNO_3$). We therefore expect that the mixed system should have lower photocatalysis than **1-Cl**, because of an inner-filter effect by **1-CN**. This contradiction is resolved by observing that **[1-CN]**$^{-\bullet}$ produced during irradiation acts as an electron donor to the CO_2 adduct made from **1(Me)** and CO_2 (Scheme 1).

Figure 8b shows the accumulation of the OER species during irradiation in three photocatalytic systems: (1) a mixed system of **1(Me)-Cl** (0.11 mM) and **1-CN** (0.11 mM), (2) **1-CN** (0.11 mM), and (3) **1(Me)-Cl** (0.11 mM). Comparison of these systems shows that, in the mixed system, the accumulated amount of the OER species was reduced compared with the system containing only **1-CN**, while **1-CN** itself was stabilized during the photocatalytic reaction.

In view of the reducing power (Table 1) and accumulation of **[1-NCS]**$^{-\bullet}$ in the reaction solution during the photocatalytic reaction using **1-NCS**, it is reasonable that **[1-NCS]**$^{-\bullet}$ also acts as an electron donor to the reaction intermediate.

We conclude that the mechanism of photocatalytic CO_2 reduction with **1-NCS** is as shown in Scheme 2. The lowest excited state ^{3}MLCT of **1-NCS** is reductively quenched by TEOA, giving the OER species **[1-NCS]**$^{-\bullet}$**.** Elimination of SCN^- from the OER species is a key step in the photocatalytic reaction. The resulting "17-electron species", for which a proposed structure is [Re(bpy$^{-\bullet}$)$(CO)_3$] (**1**),[20,21] reacts with CO_2 to give the CO_2 adduct(s). A further key role of the OER species of **1-NCS** is expected to be electron donation to the CO_2 adduct, giving rise to CO, [Re(bpy)$(CO)_3]^+$, and **1-NCS**. The eliminated anion SCN^- efficiently coordinates to the species [Re(bpy)-$(CO)_3]^+$, to recover **1-NCS**.

The action of SCN^- in this process is much greater than that of Cl^- (Figure 6b). The steady-state concentration of **1-NCS** therefore remained higher than that of **1-Cl** during irradiation (Figure 5a and 5b). This is one reason why **1-NCS** is a better photocatalyst for CO_2 reduction than **1-Cl**. In the case of **1-CN**, the nonelimination of CN^- from the OER species **[1-CN]**$^{-\bullet}$ (Figure 5c) is responsible for its absence of photocatalytic activity.

Development of More Efficient Photocatalytic Systems. New architecture for constructing more efficient photocatalytic CO_2 reduction using rhenium complexes can be based on the present mechanistic investigation in this study. The photocatalytic system should have the following properties:

(1) Efficient formation of the OER species by quenching of the ^{3}MLCT excited state by the reducing reagent.

(2) Effective production of [Re(LL$^{-\bullet}$)$(CO)_3$] by dissociation of the ligand from the OER species.

(3) Efficient reduction of the CO_2 adduct(s) by a further OER species.

(4) High-yield recovery of the starting complex by recoordination of a ligand after CO formation.

Based on these criteria, we sought to construct two-component photocatalytic systems, as follows. As a catalyst for CO_2 reduction, *fac*-[Re(bpy)$(CO)_3$(MeCN)]$^+$ (**[1-MeCN]**$^+$) was used, because it reacts with the solvent molecule to give the solvento complexes, *fac*-[Re(bpy)$(CO)_3$(S)]$^+$ (S = DMF and TEOA), in which Re−solvent bonds should be weak, within several minutes

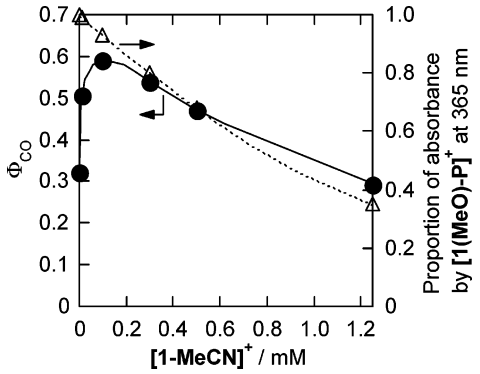

Figure 9. Dependence of Φ_{CO} (●) on the concentration of **[1-MeCN]**$^+$. A DMF−TEOA (5:1 v/v) solution containing **[1(MeO)-P]**$^+$ and **[1-MeCN]**$^+$, of which the total concentration was adjusted to 2.5 mM, was irradiated under a CO_2 atmosphere using 365-nm monochromic light of intensity 1.11×10^{-9} einstein s^{-1}. The proportion of absorbance by **[1(MeO)-P]**$^+$ at 365 nm is also shown (△).

of dissolving in a DMF−TEOA solution. The excited states have too short lifetimes to react efficiently with free TEOA, and their photocatalytic activity was low ($\Phi_{CO} = 0.04$) in the absence of a redox photosensitizer.[35]

We chose *fac*-[Re{4,4′-$(MeO)_2$bpy}$(CO)_3${$P(OEt)_3$}]$^+$ (**[1(MeO)-P]**$^+$) as a photosensitizer, because the generation quantum yield of the corresponding OER species, **[1(MeO)-P]**, is very high ($\Phi_{OER} = 1.6$)[39] and the reduction power of **[1(MeO)-P]** ($E_{1/2} = -1.67$ V vs $Ag/AgNO_3$) is high enough to reduce the solvento complexes ($E_{1/2} = -1.57$ V for the DMF complex and −1.64 V for the TEOA complex). Although only **[1(MeO)-P]**$^+$ also displayed relatively high photocatalytic activity ($\Phi_{CO} = 0.33$), the presence of **[1-MeCN]**$^+$ increased the quantum yield for CO formation. Figure 9 shows the dependence of Φ_{CO} on the ratio of **[1-MeCN]**$^+$ to **[1(MeO)-P]**$^+$ when the total concentration of the rhenium complexes is 2.5 mM. The maximum value of Φ_{CO} was 0.59, at a ratio of 1:25.

Figure 10 shows the accumulation of the OER species during the photocatalytic reaction using complexes with different ratios. Addition of **[1-MeCN]**$^+$ led to lower accumulation of **[1(MeO)-P]**; at greater concentrations of **[1-MeCN]**$^+$ than 0.1 mM (Figure 10c and d), only very low accumulation of **[1(MeO)-P]** was observed.

These results clearly show that the rate-determining process in the reduction of CO_2 by the mixed system is electron transfer from **[1(MeO)-P]** to **[1-MeCN]**$^+$ when the concentration of **[1-MeCN]**$^+$ is less than 0.1 mM under the photocatalytic reaction conditions (the light intensity was 1.11×10^{-9} einstein s^{-1}). Accumulation of the OER species lowers the photocatalytic activity of the system because of an inner-filter effect by the OER species, which has strong absorption at the irradiation wavelength, and decomposition of the accumulated **[1(MeO)-P]** due to photoexcitation. On the other hand, too high a concentration of **[1-MeCN]**$^+$ also lowered photocatalysis (Figure 9), because of another inner-filter effect by **[1-MeCN]**$^+$; direct excitation of **[1-MeCN]**$^+$ gives much lower photocatalysis as described above. It is therefore reasonable that the most efficient

(39) The extinction coefficient of **[1(MeO)-P]** at 506 nm (4900 M^{-1} cm^{-1}) was determined by the flow-electrolysis technique. TEOA can act as a two-electron donor. After photochemical oxidation of TEOA, deprotonation from its α-carbon gives an α-amino radical which has enough reducing power to reduce the rhenium(I) complexes. This is a reason why Φ_{OER} exceeds 1.

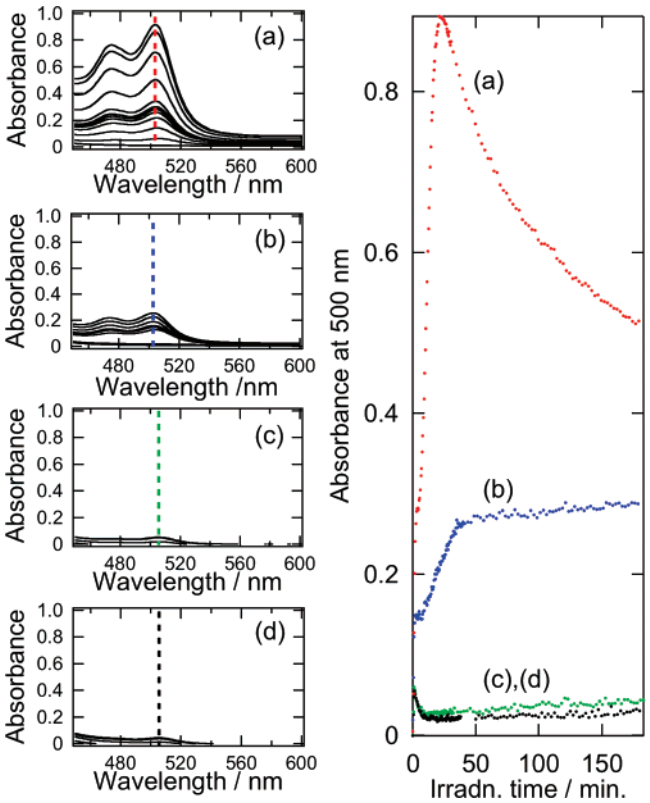

Figure 10. At left are the UV−vis spectral changes of solutions containing (a) **[1(MeO)-P]**$^+$ (2.5 mM), (b) **[1(MeO)-P]**$^+$ (2.5 mM) and **[1-MeCN]**$^+$ (0.01 mM), (c) **[1(MeO)-P]**$^+$ (2.4 mM) and **[1-MeCN]**$^+$ (0.1 mM), and (d) **[1(MeO)-P]**$^+$ (2.2 mM) and **[1-MeCN]**$^+$ (0.3 mM). To the right is the dependence of the absorbance at 500 nm on the irradiation time. Details of the photochemical reaction are shown in Figure 9.

photocatalytic CO_2 reduction was obtained by using a mixture of **[1(MeO)-P]**$^+$ and **[1-MeCN]**$^+$ in the ratio 25:1, i.e., the lowest overall inner-filter effects due to both **[1(MeO)-P]** and **[1-MeCN]**$^+$.

Conclusion

The reaction mechanism of efficient photocatalytic CO_2 reduction using *fac*-[Re(bpy)$(CO)_3$(NCS)] (**1-NCS**) has been determined as follows. The OER species of **1-NCS**, which is made by photochemical electron transfer from TEOA, plays two important roles: elimination of the SCN^- ligand gives **1**, which reacts with CO_2 to give the CO_2 adduct(s), and the OER species also works as an electron donor to the CO_2 adduct(s), leading to CO formation. Recombination of SCN^- to $\mathbf{1}^+$, which should form by CO formation, causes recovery of **1-NCS**.

Based on this mechanistic investigation, the most efficient photocatalytic system for CO_2 reduction in the reported homogeneous photocatalysts has been developed, i.e., the 25:1 mixture of **[1(MeO)-P]**$^+$ as photosensitizer and **[1-MeCN]**$^+$ as catalyst, for which the quantum yield of CO formation is 0.59 at an irradiated light intensity of 1.11×10^{-9} einstein s^{-1}.

Supporting Information Available: HPLC chromatograms of the reaction solutions after the photocatalytic reaction, ratios between **1-Cl** and **1-NCS** at photostationary states, and time profiles of **[1-NCS]**$^{-\bullet}$ during the photocatalytic reaction in the presence of excess amount of Et_4NCl. This material is available free of charge via the Internet at http://pubs.acs.org.

JA077752E